

# Structural Cost Optimization using Interval FEM

Simi Rose George

**Abstract**—In the conventional (deterministic) FEM, the possibility of failure is reduced to acceptably small levels by factors of safety based on judgment-derived from past successful and unsuccessful performances. By contrast, the interval FEM can be applied in situations where it is not possible to get reliable probabilistic characteristics of the structure. This is important in concrete structures, wood structures, composite structures, biomechanics and in many other areas. The goal of the Interval Finite Element Method is to find upper and lower bounds of different characteristics of the model (e.g. stress, displacements, yield surface etc.) and use these results in the design process. Deflection, bending moment & shear forces of structure are computed using MATLAB coding. And designed a structure using modified IS code equations. The cost of structure is calculated and compared with the cost from conventional design.

**Index Terms**—Interval FEM,Optimiation,Space frame equations,RC in FEM, Wind load, Structural cost, Earthquake load, Uncertainties

## 1 INTRODUCTION

Little attention has been paid to the cost optimization problem, particularly of realistic three-dimensional structures. Cost optimization is becoming a priority in all civil engineering projects, manufacturing and construction organizations.

Interval FEM is a method to incorporate all the uncertain parameters. These are modelled by using the interval theory and solved for responds by interval arithmetic [5].

Goal of a structural engineer is to achieve required strength for frame structure with minimum cost in every design. A new method is developed in the paper to optimize the initial cost of structure using fuzzy logic in FEM. Instead of using the interval arithmetic directly, the special algorithm developed [4] by GuoShu-xiang& Lu Zhen-zhou is used for optimal performance of MATLAB coding.An apartment is selected for illustration of the method. The steps involved are demonstrated in Fig.1

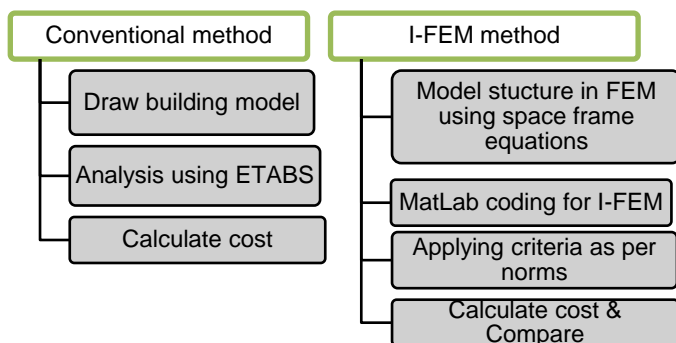


Fig. 1 Methodology followed

## 2 CONVENTIONAL DESIGN

The building was modelled and analysed conventionally in Etabs. The deformation of the frame analysed using the software is shown in Fig.2. Cost of the structure from this is calculated to compare the degree of optimization by IFEM

## 3 FEM DESIGN

The complete frame is discretised and each element is considered as space frames. Due to symmetry only half of the structure analysed. This reduces the computational cost. The element numbering is given in Table.1 and node numbering in Table.2.

ment numbering is given in Table.1 and node numbering in Table.2.

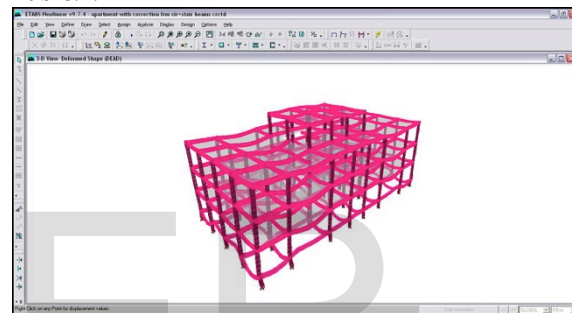


Fig. 2Etabs analysis

TABLE.1  
ELEMENT NUMBERIG

Type of element	Floor	Number of elements	Element numbering
Column	Base	24	1 - 24
	Plinth	24	25 - 48
	Story 1	24	49 - 72
	Story 2	24	73 - 96
X- Beams	Roof	08	97 - 104
	Plinth	21	105 - 125
	Story 1	20	126 - 145
	Story 2	20	146 - 165
	Roof	20	166 - 185
Y- Beams	Roof Top	06	186 - 191
	Plinth	16	192 - 207
	Story 1	16	208 - 223
	Story 2	16	224 - 239
	Roof	16	240 - 255
Roof Top	04	256 - 259	
Total		259	

TABLE.2  
NODE NUMBERING

Floor	Number of Nodes	Node Numbers
Base	24	1 - 24
Plinth	24	25 - 48
Story 1	25	49 - 72 & 129
Story 2	25	73 - 96 & 130
Roof	25	97 - 120 & 131
Roof Top	08	122 - 128
Total		131

Dimensions of all the elements are taken from the ETABS analysis as this is used as reference to our programming initially and optimized and reduced the sizes. The displacements are compared to check the program and then proceed to the optimization.

$$k_l = \begin{bmatrix} EA/L & 0 & 0 & 0 & 0 & 0 & -EA/L \\ 0 & 12EI_r/L^3 & 0 & 0 & 0 & 6EI_r/L^2 & 0 \\ 0 & 0 & 12EI_s/L^3 & 0 & -6EI_s/L^2 & 0 & 0 \\ 0 & 0 & 0 & GJ/L & 0 & 0 & 0 \\ 0 & 0 & -6EI_s/L^2 & 0 & 4EI_s/L & 0 & 0 \\ 0 & 6EI_r/L^2 & 0 & 0 & 0 & 4EI_r/L & 0 \\ -EA/L & 0 & 0 & 0 & 0 & 0 & EA/L \\ 0 & -12EI_r/L^3 & 0 & 0 & 0 & -6EI_r/L^2 & 0 \\ 0 & 0 & -12EI_s/L^3 & 0 & 6EI_s/L^2 & 0 & 0 \\ 0 & 0 & 0 & -GJ/L & 0 & 0 & 0 \\ 0 & 0 & 6EI_s/L^2 & 0 & 2EI_s/L & 0 & 0 \\ 0 & 6EI_r/L^2 & 0 & 0 & 2EI_r/L & 0 & 0 \end{bmatrix}$$

$$3.1 \begin{bmatrix} S & 0 & 0 & 0 & 0 & 0 \\ p & -12EI_r/L^3 & 0 & 0 & 0 & 6EI_r/L^2 \\ a & 0 & -12EI_s/L^3 & 0 & -6EI_s/L^2 & 0 \\ c & 0 & 0 & -GJ/L & 0 & 0 \\ e & 0 & 6EI_s/L^2 & 0 & 2EI_s/L & 0 \\ f & -6EI_r/L^2 & 0 & 0 & 0 & 2EI_r/L \\ r & 0 & 0 & 0 & 0 & -6EI_r/L^2 \\ a & 0 & 12EI_s/L^3 & 0 & 6EI_s/L^2 & 0 \\ m & 0 & 0 & GJ/L & 0 & 0 \\ e & 0 & 6EI_s/L^2 & 0 & 4EI_s/L & 0 \\ & -6EI_r/L^2 & 0 & 0 & 0 & 4EI_r/L \end{bmatrix}$$

**equations**

Using space frame equations [8] the element stiffness matrix and force vector are calculated as follows:

- Where E Young's modulus
- G Shear modulus
- A Area of cross section
- J Torsional constant
- I<sub>p</sub> Polar moment of inertia
- I<sub>s</sub> Moment of inertia of cross section about s axis
- I<sub>r</sub> Moment of inertia of cross section about r axis
- L Length of element

$$r_l^T = \int_0^L (q_s \ q_r) N^T dt \tag{1}$$

Now the displacement in local coordinates can be transformed to global using the equation (2).

$$d_l = Td$$

$$T = \begin{pmatrix} H & 0 & 0 & 0 \\ 0 & H & 0 & 0 \\ 0 & 0 & H & 0 \\ 0 & 0 & 0 & H \end{pmatrix} \tag{2}$$

$$H = \begin{pmatrix} l_t & m_t & n_t \\ l_s & m_s & n_s \\ l_r & m_r & n_r \end{pmatrix}$$

By substituting the transformation equation in FEM equation in local coordinates, equation (3) is derived

$$T^T k_l T d = T^T r_l \tag{3}$$

**3.2 Boundary Condition**

Because of large dimensions, the floor system within its own plane is essentially rigid and known as a rigid diaphragm. Thus individual frames in a building do not behave as their isolated counterparts.

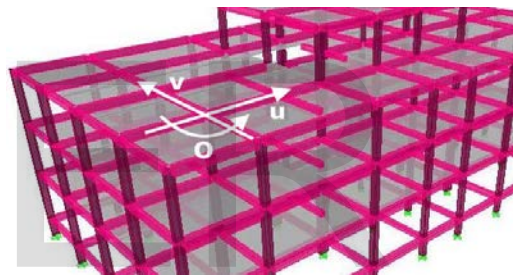


Fig. 3 Rigid diaphragm constrains

With the assumption of an in-plane rigid floor system, the two displacements in x and y directions (u and v) and a rotation about the z axis (o) are constrained as given in Eq.(4)

$$\begin{bmatrix} u_i \\ v_i \\ o_i \end{bmatrix} = \begin{bmatrix} 1 & 0 & -(y_i - y_m) \\ 0 & 1 & x_i - x_m \\ 0 & 0 & 1 \end{bmatrix} \begin{bmatrix} u_m \\ v_m \\ o_m \end{bmatrix} \tag{4}$$

Where x<sub>i</sub> and y<sub>i</sub> are the coordinates of node i

When creating frame models using centreline dimensions, the joint zone with these large member sizes is fairly large. Very little deformations are expected within this joint zone.

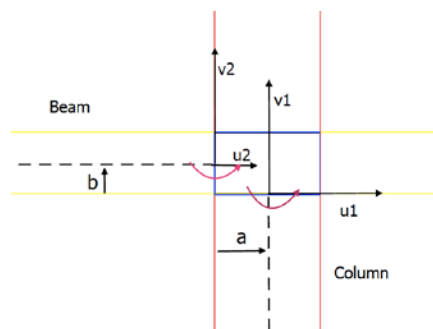


Fig. 4 Rigid joint constrains

Thus the Eq.(5) is used to define the rigid joint zone

$$\begin{aligned} \theta_1 &= \theta_2; \quad u_1 = u_2 + b\theta_2; \\ v_1 &= v_2 + a\theta_2 \end{aligned} \tag{5}$$

After incorporating these constraints using Langrangian multiplier, the rest of the analysis follows the standard procedures of space frame.

It is assumed that all the nodes in the base are fixed and thus the displacements are zero. And these can be enforced directly. However, other constraints of rigid diaphragm and rigid joint are incorporated using Langrangian multiplier method.

### 3.3 Loads

All the area loads are converted using the well-known trapezoidal method and applied on beams. The earthquake and wind loads are not taken in the initial program. These are included in IFEM as uncertainties of loads.

## 4 INTERVAL FEM

Initial coding has done for FEM and modified it to include the uncertainties.

### 4.1 Load Uncertainties

Major load uncertainty comes from wind and earthquake. The wind load [12] is applied on all the peripheral frames as per the details given below:

Basic wind speed in the place building located,  $V_b = 35 \text{ m/s}$

The apartment building can be grouped under all general building and structure so should be designed for 50 years of design life. And thus the risk coefficient,  $k_1 = 1$

The terrain factor is interpolated for building height,  $k_2 = 0.605$

The ground is plane and thus the topography factor,  $k_3 = 1$

So the design wind speed,  $V_z = k_1 k_2 k_3 V_b$

Using the above equation, the wind speed is calculated as 21.18 m/s. And the design wind pressure is 269 N/m<sup>2</sup> using the equation

Design wind pressure,  $P_d = 0.6 V_z^2$

Similarly, the wind pressure at different heights are calculated and found these are following a parabolic shape as shown in Fig.5

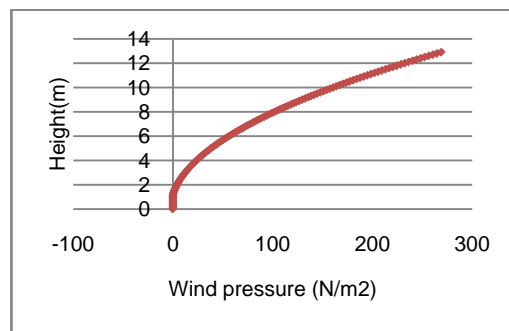


Fig. 5 Wind Pressure variation

This pressure is applied on the peripheral areas and thus converted to line loads applied in lateral direction to the peripheral beams and columns using the trapezoidal method. And the wind pressure is not applied simultaneously on all the 04 sides. It is applied in each side and selected the largest value of shear and moment.

During an earthquake, ground motions occur in a random fashion, both horizontally and vertically, in all the directions radiating from the epicenter. These ground motions cause structures to vibrate and induce internal forces on them. These seismic dynamic loads are represented as equivalent lateral static loads in Fig.6

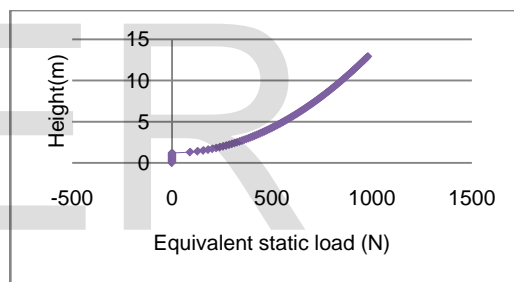


Fig. 6 Earthquake load variation

It is general assumption that the earthquake and wind effects do not coexist. So both are applied separately and selected the largest values.

### 4.2 Uncertainties in material properties

The properties are calculated from experiments and consolidate in Table.3

TABLE.3  
MATERIAL PROPERTIES

Property	Mean value	Standard deviation	Interval
Modulus of Elasticity Steel Fe415	1.999 x 10 <sup>11</sup>	4.998x 10 <sup>9</sup>	[1.899x10 <sup>11</sup> - 2.099x10 <sup>11</sup> ]
Modulus of Elasticity Concrete M25	2.482 x 10 <sup>10</sup>	9.928x 10 <sup>8</sup>	[2.283x10 <sup>10</sup> - 2.681x10 <sup>10</sup> ]

Modulus of Elasticity Concrete M20	of -	$2.225 \times 10^{10}$	$1.034 \times 10^9$	$[2.018 \times 10^{10}$ $2.442 \times 10^{10}]$
Modulus of Elasticity Concrete M15	of -	$1.929 \times 10^{10}$	$1.118 \times 10^9$	$[1.705 \times 10^{10}$ $2.153 \times 10^{10}]$
Poisson's ratio-Steel Fe415		0.285	$7.5 \times 10^{-3}$	$[0.27 \ 0.30]$
Poisson's ratio-Concrete		0.14	$2.0 \times 10^{-3}$	$[0.10 \ 0.18]$

Shear stress at critical section to be checked for shear reinforcement.

## 5 RESULT

After analysing the structure in MATLAB using I-FEM the following observations are obtained

- More size minimization occurred for the interior elements
- The reduction took place more in concrete than in steel

## 6 CONCLUSION

For the selected structure the cost has reduced from 22.9 lakhs to 18.3 lakhs, less by 20%. Thus the method takes care of the uncertainties and give an optimum design. The overestimation due to FOS leads to 20% more cost.

Since the uncertainty is more in case of concrete than steel, higher value of Factor of Safety is used for concrete in conventional design. This leads to more weight and thus more dead load.

The wind load acts only on peripheral elements of structure. However, in conventional design, the the SOF for all the uncertainties are applied together to all the elements and this leads to overestimation. The MATLAB coding has done for a particular frame. However, with some simple modification it can be extended to any building structure.

## 4.3 BENDING MOMENT AND SHEAR FORCE

All the 06 elemental displacements ( $u, v, w, \theta, \phi, \psi$ ) along the length of frame can be formulated from the nodal displacements. All these are functions of  $t$ , distance from node 1 of the element along  $t$ -axis. The bending moments, shear forces and twisting moments are given in equation 6,7 & 8 respectively.

$$M_s(t) = -EI_s \left( \frac{d^2 w}{dt^2} \right); 0 \leq t \leq L \quad (6)$$

$$M_r(t) = EI_r \left( \frac{d^2 v}{dt^2} \right); 0 \leq t \leq L$$

$$V_s(t) = -EI_s \left( \frac{d^3 w}{dt^3} \right); 0 \leq t \leq L \quad (7)$$

$$V_r(t) = EI_r \left( \frac{d^3 v}{dt^3} \right); 0 \leq t \leq L$$

$$M_t(t) = GJ \frac{d\psi}{dt} \quad (8)$$

$$\text{Where } \psi(t) = \left( 1 - \frac{t}{L} \quad \frac{t}{L} \right) \left( \frac{d_4}{d_{10}} \right); 0 \leq t \leq L$$

However we are interested for the maximum values of the moments and forces. For the simply supported beams with equally distributed load, the maximum moments are at the centre ( $t = L/2$ ) and the shear forces the critical sections are at a distance of  $d$ , the depth of beam, from either ends. The axial forces are same throughout the length.

## 4.4 Design Criteria

The HYSD Fe-415 steel is used for the complete frame. The maximum possible bending moment, axial forces are limited as per the Equation 9 and 10 respectively. And these are derived from maximum yield strain

$$M_{limit} = 0.207 F_{ck} b d^2 \quad (9)$$

$$F_{limit} = 0.67 F_{ck} A_c + F_y A_{sc} \quad (10)$$

## REFERENCES

- [1] Edoardo Patelli, H. Murat Panayirci, Matteo Broggi, Barbara Goller, Pierre Beaupaire, Helmut J. Pradlwarter, Gerhart I. Schuefler, "Finite Elements in Analysis and Design", General purpose software for efficient uncertainty management of large finite element models, vol. 51, pp. 31-48, 2012.
- [2] Egor P. Popov, "Engineering Mechanics of Solids", 2<sup>nd</sup> edn, Prentice-Hall India, New Jersey, 2004.
- [3] Florentin Smarandache, "Interval Linear Algebra", 1<sup>st</sup> edn, Kappa & Omega, Glendale USA, 2010.
- [4] Guo Shu-xiang, Lu Zhen-zhou, "Interval FEM", interval arithmetic and static interval Finite element method, vol. 22, pp. 1391-1396, Dec 2001.
- [5] Hao Zhang, "Structural Safety", Interval importance sampling method for finite element-based structural reliability assessment under parameter uncertainties, vol. 38, pp. 1-10, 2012.
- [6] IIT Madras, "Finite Element Method", <http://nptel.ac.in/courses/105106051/>
- [7] Kamal C. Sarma, Hoijat Adeli, "Journal of structural engineering", Cost optimization of concrete structures, vol. 5, pp. 570-578, 1998.
- [8] M. Asghar Bhatti, "Fundamental Finite Element Analysis and Applications", 1<sup>st</sup> edn, Wiley India Pvt. Ltd., New Delhi, 2013.

- [9] O.C.Zienkiewicz&R.L.Taylor, "The Finite Element Method", 5<sup>th</sup>edn, Butterworth Heinemann, Barcelona Spain, 2000.
- [10] Paul G. Tucker, "Computation of Unsteady Interval Flows: Fundamental Methods with Case Studies", 1<sup>st</sup>edn, Google Books, Glendale USA, 2010.
- [11] Raad A. Abdul-Aziz, M.ASCE, "Embedded Steel Bars Simulation in Reinforced Concrete Using Three-Dimensional Finite Elements", Analysis and computation specialty conference, vol.1, pp. 1-15, 2006.
- [12] PanneerSelvam and Zu-Qing Qu, "Adaptive Finite Element Method for Wind Engineering Problems", Structure 2001, vol. 51, pp. 31-48, 2012.
- [13] Sanjaya K. Patro, R. PanneerSelvam, Harold Bosch, "Adaptive h-finite element modeling of wind flow around bridges", Engineering Structures , vol. 48, pp. 569-577, 2013.
- [14] Wikipedia, "hp-FEM", <https://en.wikipedia.org/wiki/Hp-FEM>

IJSER